Emissivity-Limited Implicit Monte Carlo

Ryan T. Wollaeger, Mathew A. Cleveland, HyeongKae Park

Los Alamos National Laboratory, P.O. Box 1663, MS D409, Los Alamos, NM, 87545
wollaeger@lanl.gov

INTRODUCTION

Implicit Monte Carlo (IMC) [1] is a widely used method for solving the equations of radiative transfer in local thermodynamic equilibrium (LTE). A long standing problem in IMC is the tendency for Marshak waves to over-propagate in problems with optically thick spatial cells and small time steps. This so-called "teleportation error" [2] is a result of the IMC equations not converging to a valid discretization of the equilibrium-diffusion equation. Teleportation error is typically mitigated by reconstructing the emission ("source tilting") and sampling source particle positions with the resulting profiles. Source tilting does not necessarily permit IMC to retain the diffusion limit [3]. It was recently shown that forcing continuity in the reconstructed temperature profile permits the diffusion limit to be obtained [4].

Alternatively, finite element and node-centered discretizations of the material-energy equation have been shown to retain the equilibrium diffusion limit in 1D [5, 6, 7]. These methods do not require reconstructed emission profiles to sample Monte Carlo particle positions, since node temperatures or emission are obtained directly from the material-energy equation. However, in order to accurately update node-centered temperatures, a sufficient number of particles must be present in each cell. Moreover, for LD IMC [6], implicit capture absorption requires basis-weighted integration along particle paths.

Here, we present a modification to the IMC method that retains the equilibrium diffusion limit at small time steps without introducing finite elements or reconstructions for emission. Specifically, we introduce a diffusion-informed emissivity limiter on flux at cell faces, similar to the albedo condition used in Discrete Diffusion Monte Carlo (DDMC) [8]. For Monte Carlo, this limiter is a transmission probability between cells; particles that do not sample transmission get isotropically reflected to their current cell. We discuss the derivation of the emissivity limiter in 1D planar geometry, but note the method is straightforward to extend to multiple dimensions or curvilinear geometry, since it is an albedo condition at cell surfaces. The transmission probability derived here is appropriate for cell faces in 2D or 3D Cartesian geometry.

DIFFUSION EMISSIVITY LIMITER

The 1D, planar, LTE, grey, purely absorbing radiative transfer equations are

$$\frac{1}{c}\frac{\partial I}{\partial t} + \mu\frac{\partial I}{\partial x} = \frac{1}{2}\sigma acT^4 - \sigma I \quad , \tag{1}$$

and

$$C_v\frac{\partial T}{\partial t} = \int_{-1}^{1}\sigma I d\mu - \sigma acT^4 \quad , \tag{2}$$

where t is time, x is the spatial coordinate, μ is the direction cosine, I is radiation intensity, T is material temperature, c is the speed of light, a is the radiation constant, σ is absorption opacity, and C_v is the heat capacity. Semi-implicitly discretizing in time, the corresponding IMC equations are [1]

$$\frac{1}{c}\frac{\partial I}{\partial t} + \mu\frac{\partial I}{\partial x} = \frac{1}{2}f_n\sigma_n acT_n^4 - \sigma_n I + \frac{1}{2}(1-f_n)\sigma_n\int_{-1}^{1} I d\mu' \quad , \tag{3}$$

$$C_{v,n}\frac{\partial T}{\partial t} = \int_{-1}^{1} f_n\sigma_n I d\mu - f_n\sigma_n acT_n^4 \quad , \tag{4}$$

and

$$f_n = \frac{1}{1+\alpha\beta_n\sigma_n c\Delta t_n} \quad , \tag{5}$$

where subscript n denotes the beginning of time step n, α is a time-centering parameter, $\beta_n = 4aT_n^3/C_{v,n}$, and $\Delta t_n = t_{n+1} - t_n$.

Integrating Eq. (3) in angle and over a spatial cell, and assuming piecewise-constant material data,

$$\frac{1}{c}\frac{\partial \phi_i}{\partial t} + \frac{F_{i+1/2} - F_{i-1/2}}{\Delta x_i} = f_{n,i}\sigma_{n,i}acT_{n,i}^4 - f_{n,i}\sigma_{n,i}\phi_i \quad , \tag{6}$$

where subscript i denotes cell index, subscripts $i \pm 1/2$ denote cell face values, $\Delta x_i = x_{i+1/2} - x_{i-1/2}$, and

$$\phi_i = \frac{1}{\Delta x_i}\int_{x_{i-1/2}}^{x_{i+1/2}}\int_{-1}^{1} I(x,\mu)d\mu dx \quad , \tag{7}$$

$$F_{i\pm1/2} = \int_{-1}^{1}\mu I(x_{i\pm1/2},\mu)d\mu \quad . \tag{8}$$

Provided the cell is of sufficient optical depth, we may approximate Eq. (8) with a discretized form of Fick's Law [8],

$$F_{i-1/2} = -\frac{2}{3\sigma^+_{n,i-1/2}}\frac{\phi_i - \phi_{i-1/2}}{\Delta x_i} \quad , \tag{9}$$

where, as in [8], superscript + denotes evaluation to the right of face $i-1/2$. To evaluate $\phi_{i-1/2}$, we invoke the general form of the asymptotic diffusion-limit boundary condition [9, 8],

$$2\int_0^1 W(\mu)I^-_{i-1/2}(\mu)d\mu = \phi_{i-1/2} - \frac{2\lambda}{\sigma^+_{i-1/2}}\frac{\phi_i - \phi_{i-1/2}}{\Delta x_i} \quad , \tag{10}$$

where $W(\mu)$ and λ are typically estimated to be $\mu + 3\mu^2/2$ and 0.7104, respectively. Instead of 0.7104, the value of λ is set to recover the DDMC stencil for scalar flux in "interior" [8] cells,

$$\lambda = \frac{1}{2}\sigma^-_{i-1/2}\Delta x_{i-1} \quad . \tag{11}$$

Incorporating Eqs. (9)-(11) into Eq. (6),

$$\frac{1}{c}\frac{\partial \phi_i}{\partial t} + \frac{F_{i+1/2}}{\Delta x_i} + \sigma_{L,i}\phi_i - \frac{1}{\Delta x_i}\int_0^1 P_{i-1/2}(\mu)\mu I^-_{i-1/2} d\mu = f_{n,i}\sigma_{n,i} acT^4_{n,i} - f_{n,i}\sigma_{n,i}\phi_i \ , \quad (12)$$

where $\sigma_{L,i}$ is the left leakage opacity as described by [8], and

$$P_{i-1/2}(\mu) = 2\sigma_{L,i}\Delta x_i \frac{W(\mu)}{\mu} = \frac{4}{3}\frac{1}{\sigma^+_{i-1/2}\Delta x_i + \sigma^-_{i-1/2}\Delta x_{i-1}}\left(1 + \frac{3}{2}\mu\right) \ . \quad (13)$$

If cell $i-1$ is sufficiently optically thick, $I^-_{i-1/2}$ can be approximated as $\phi_{i-1}/2$, so that

$$\frac{1}{\Delta x_i}\int_0^1 P_{i-1/2}(\mu)\mu I^-_{i-1/2} d\mu = \sigma_{L,i}\phi_{i-1}\int_0^1 W(\mu)d\mu = \frac{\Delta x_{i-1}}{\Delta x_i}\sigma_{R,i-1}\phi_{i-1} \ . \quad (14)$$

Substituting the right side of Eq. (14) into Eq. (12) gives the 0th moment of the discrete transport equation with the standard DDMC stencil applied to face $i-1/2$. It is straightforward to find the corresponding sequence of equations for face $i+1/2$.

Particle Algorithm

Emissivity-limited IMC is nearly identical to standard IMC, except that an albedo is applied at each cell face, and that *source particle positions do not need to be sampled from a non-constant sub-cell emission profile.* Thus, particle positions are sampled as

$$x = x_{i-1/2} + \xi\Delta x_i \ , \quad (15)$$

where $\xi \in [0,1]$ is a uniformly sampled random number.

We apply Eq. (13) as a transmission probability for IMC particles going in a cell with $\sigma_{n,i-1}\Delta x_{i-1} > \tau_{\text{th}}$, incident on a cell with $\sigma_{n,i}\Delta x_i > \tau_{\text{th}}$, where τ_{th} is a threshold optical depth. Thus, the true transmission probability, $P^*_{i-1/2}(\mu)$, for IMC particles is

$$P^*_{i-1/2}(\mu) = \begin{cases} P_{i-1/2}(\mu) & , \sigma_{n,i}\Delta x_i > \tau_{\text{th}} \text{ and } \sigma_{n,i-1}\Delta x_{i-1} > \tau_{\text{th}} \\ 1 \ , \ \text{otherwise} & . \end{cases} \quad (16)$$

Preliminary numerical testing here indicates an optimal value of τ_{th} is ~10-20.

NUMERICAL RESULTS

Marshak Wave

We test the emissivity limiter on a standard optically thick Marshak wave problem, with coarse cell resolution. This problem has: a domain of 0.25 cm with 10 uniform cells, a time span of 20 ns with 2000 time steps, a 1 keV isotropic left surface source, vacuum boundary conditions, 1 eV uniform initial temperature, $\sigma = 1000/T^3$ cm^{-1}, where T is in keV, $C_v = 3\times10^{15}$ erg/keV/cm^3, and 100000 source particles per time step. This problem does not test τ_{th} in Eq. (16), since it is set lower than the minimum optical depth each cell can reach (25).

Figure 1 has a plot of material temperature at 20 ns. Plotted for comparison are the temperature solutions for analytic equilibrium diffusion, standard IMC with a source tilt reconstruction linear in T^4, DDMC, and LD IMC with constant sub-cell opacity ("LD-0").

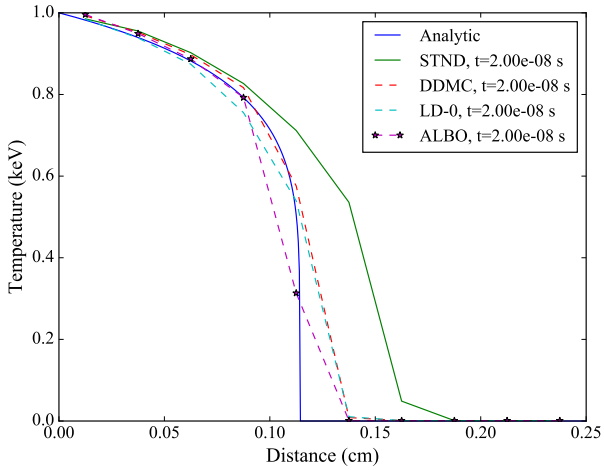

Fig. 1: Analytic (solid blue), standard IMC (STND, solid green), DDMC (dashed red), LD-0 IMC (dashed light blue), and emissivity-limited IMC (ALBO, dot-dashed purple) material temperature profiles for the Marshak wave problem at 20 ns.

We also perform a resolution test in space and time to obtain a preliminary estimate of the optimal τ_{th} for this Marshak wave test. With $\tau_{\text{th}} \in \{5, 10, 20\}$, we examine the spatial L_1 norm relative to the analytic diffusion solution at 10 ns. Each τ_{th} test is simulated out to 10 ns with four resolutions: 10 cells and 125 time steps ("1x"), 20 cells and 250 time steps ("2x"), 40 cells and 500 time steps ("4x"), 80 cells and 1000 time steps ("8x"). Otherwise, the problem specification is unchanged.

The following table has the L_1 norms for each τ_{th} and each resolution. We find that the 2x resolution has relatively large error for $\tau_{\text{th}} \in \{5, 10\}$, which corresponds to the wavefront lagging the analytic solution. On the other hand, at $\tau_{\text{th}} = 20$ the limiter permits some teleportation error at $4x$ and $8x$ resolutions. These results suggest that an optimal implementation of τ_{th} may generally be formulaic.

Spatial L_1 norm relative to analytic solution, at 10 ns.

τ_{th} \ Resolution	1x	2x	4x	8x
$\tau_{\text{th}} = 5$	0.11	0.19	0.22	0.07
$\tau_{\text{th}} = 10$	0.11	0.19	0.04	0.03
$\tau_{\text{th}} = 20$	0.11	0.06	0.08	0.05

Hat Opacity Problem

Next, we consider a version of the standard Larsen problem [10], which consists of: a 1 cm domain with 40 uniform cells, a duration of 80 ns with 2000 time steps, a 1 keV isotropic left surface source, vacuum boundary conditions, 0.001 eV uniform initial temperature, $\sigma = 10^{-8}/T^3$ cm^{-1} from 0 to .25 cm, $1000/T^3$ cm^{-1} from .25 to .4 cm, $10^{-8}/T^3$ cm^{-1} from .4 to 1 cm, where T is in keV, $C_v = 3 \times 10^{15}$ erg/keV/cm^3 heat capacity, and 100000 source particles per time step.

In this problem, at the given spatial resolution, the temperature in the optically thin region furthest away from the source is sensitive to how teleportation error is mitigated in the optically thick region. This sensitivity is illustrated in Figs. 2a-2c, where spatial temperature profiles from emissivity-limited IMC, with $\tau_{\text{th}} \in \{5, 10, 20\}$, are shown. For comparison, each plot in Fig. 2 also has a temperature profile from LD-0 IMC. At $\tau_{\text{th}} = 5$, which has a threshold temperature of ∼0.37 eV, the first branch of Eq. (16) (Eq. (13)) is evidently over-applied near the first interface between optically thin and thick regions, which keeps the energy transmission too low. The converse occurs for $\tau_{\text{th}} = 20$, which, relative to the range of temperatures in the problem, has a modestly different threshold temperature of ∼0.23 eV. However, the small threshold temperatures may be misleading: since the optical depth is low in the first region, high-energy photons from the surface source are not strongly attenuated. Consequently, in the optically thick region, the temperature difference due to different τ_{th} can be larger than the difference in threshold temperatures.

SUMMARY

Teleportation error has been a persisting problem in IMC and Symbolic IMC [11], and the equivalent pathology has long been recognized in deterministic methods, motivating higher order solutions to the transport equation. For Monte Carlo, solutions to eliminate teleportation error so far have included: continuous material temperature reconstruction for source tilting [4], finite elements [5, 6], and node-centered stencils [7].

We have presented an alternative method to eliminate teleportation error in IMC simulations. The method limits the amount of IMC particles that can be transmitted across cell faces by applying a diffusion-theory based albedo condition between neighboring optically thick cells.

We have also performed an analysis in 1D that verifies emissivity-limited IMC converges asymptotically to the discrete diffusion limit, but defer this for a future publication. In this future work, we will also investigate a multigroup implementation of the emissivity-limiter. An open question for the method concerns the optimal determination of the threshold optical depth parameter, τ_{th}.

ACKNOWLEDGMENTS

This work was performed under U.S. government contract DE-AC52-06NA25396 for Los Alamos National Laboratory, which is operated by Los Alamos National Security, LLC, for the U.S. Department of Energy.

REFERENCES

1. J. A. FLECK, JR. and J. D. CUMMINGS, "An implicit Monte Carlo scheme for calculating time and frequency dependent radiation transport," *J. Comput. Phys.*, **8**, 313 (1971).
2. M. S. MCKINLEY, E. D. BROOKS, III, and A. SZŐKE, "Comparison of implicit and symbolic implicit Monte Carlo line transport with frequency weight vector extension," *J. Comput. Phys.*, **189**, 330 (2003).
3. J. D. DENSMORE, "Asymptotic analysis of the spatial discretization of radiation absorption and re-emission in Implicit Monte Carlo," *J. Comput. Phys.*, **230**, 1116 (2011).
4. R. P. SMEDLEY-STEVENSON and R. G. MCCLARREN, "Asymptotic diffusion limit of cell temperature discretisation schemes for thermal radiation transport," *J. Comput. Phys.*, **286**, 214 (2015).
5. E. D. BROOKS, III, A. SZŐKE, and J. D. L. PETERSON, "Piecewise linear discretization of Symbolic Implicit Monte Carlo radiation transport in the difference formulation," *J. Comput. Phys.*, **220**, 471 (2006).
6. R. T. WOLLAEGER, A. B. WOLLABER, T. J. URBATSCH, and J. D. DENSMORE, "Implicit Monte Carlo with a linear discontinuous finite element material solution and piecewise non-constant opacity," *Journal of Computational and Theoretical Transport*, **45**, *1-2*, 123–157 (2016).
7. A. R. LONG and R. G. MCCLARREN, "A node-centered IMC discretization with correct diffusion limit behavior," in "ICTT 25 - 25th International Conference on Transport Theory, Monterey, California, 16-20 October 2017," (2017).
8. J. D. DENSMORE, T. J. URBATSCH, T. M. EVANS, and M. W. BUKSAS, "A hybrid transport-diffusion method for Monte Carlo radiative-transfer simulations," *J. Comput. Phys.*, **222**, 485 (2007).
9. G. HABETLER and B. MATKOWSKY, "Uniform asymptotic expansions in transport theory with small mean free paths, and the diffusion approximation," *Journal of Mathematical Physics*, **16**, *4*, 846–854 (1975).
10. B. CHANG, "A deterministic photon free method to solve radiation transfer equations," *Journal of Computational Physics*, **222**, *1*, 71–85 (2007).
11. E. D. BROOKS, III, "Symbolic Implicit Monte Carlo," *J. Comput. Phys.*, **83**, 433 (1989).

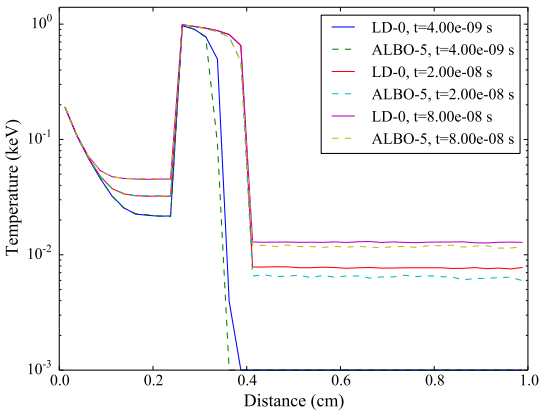

(a)

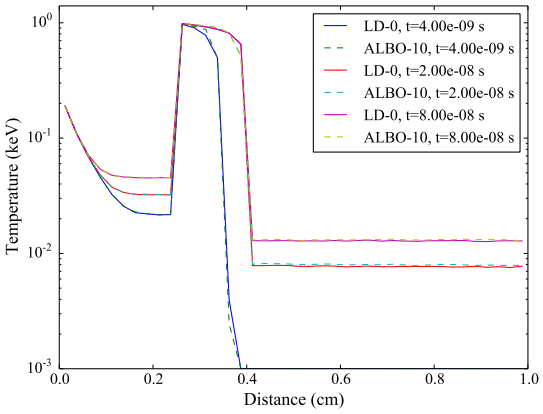

(b)

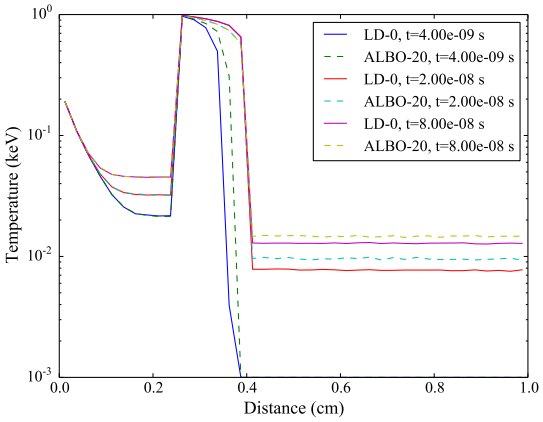

(c)

Fig. 2: Material temperature profiles for the hat opacity problem. In Figs. 2a, 2b, 2c, emissivity-limited IMC with a τ_{th} =5, 10, and 20, respectively (dashed), along with LD-0 IMC (solid).